

STEFANO BORGANI

Department of Physics, University of Trieste

## Cosmological Simulations of a Large Sample of Massive Galaxy Clusters

## The simulation code

Using the CPU time allocated for a IS CRA type B project, we have carried out cosmological simulations of 29 Lagrangian regions extracted around as many clusters of galaxies identified within a low-resolution N-body cosmological simulations.

In this Section we introduce the simulation code. Simulations have been carried out using the Tree-PM SPH GADGET-3 code, a newer and more efficient version of the previous GADGET-2 code (Springel 2005). The difference between the two versions resides mainly in the different algorithm adopted for domain decomposition. Both versions of the code use segments of the space-filling Peano-Hilbert curve to decide the particles to be assigned to different processors. Unlike GADGET-2, the newest GADGET-3 version allows each processor to be assigned also disjointed segments of the Peano-Hilbert curve. This turns into a substantial improvement of the work-load balance assigned to the different processors, especially for simulations, like those presented here, in which the computation cost is largely concentrated within a quite small fraction of the physical volume of the computational domain.

## The sets of simulations

We provide here below a short description of the initial conditions, while a more detailed presentation is provided in the paper by Bonafede *et al.* (2011). The parent DM simulation follows  $\Lambda$ CDM particles within a simulation box having a co-moving side of  $1h^{-1}\text{Gpc}$ . The cosmological model assumed is a flat  $\Lambda$ CDM one, with parameters consistent with the latest data from WMAP CMB anisotropies (Komatsu *et al.* 2010). The selected Lagrangian regions have been chosen so that 24 of them are centered around the 24 most massive clusters found in the cosmological volume, all having virial mass  $M_{\text{vir}} < 10^{15}h^{-1}M_{\odot}$ . Further five regions have been chosen around clusters in the mass range  $M_{\text{vir}} \simeq (1-7) \times 10^{14}h^{-1}M_{\odot}$ .

Within each Lagrangian region we increased mass resolution and added the relevant high-frequency modes of the power spectrum, following the Zoomed Initial Condition (ZIC) technique (Tormen *et al.* 1997). Initial conditions for hydrodynamic simulations have been generated by splitting each particle within the high-resolution region into a DM and a gas particle, having mass ratio such to reproduce the cosmic baryon fraction. Outside high-resolution regions resolution is progressively degraded, so as to save computational time, while preserving a correct description of the large-scale tidal field. We generated initial conditions at different, progressively increasing, resolution. Using an iterative procedure, we have shaped each high-resolution Lagrangian region in such a way that no low-resolution particle contaminates the central "zoomed in" halo at redshift  $z=0$  at least out to 5 virial radii of the central cluster. This implies that each region is sufficiently large to contain more than one interesting cluster with no "contaminants" out to at least one virial radius. In total, we find  $\simeq 140$  clusters with  $M_{500} > 5 \times 10^{13}h^{-1}M_{\odot}$  out of which about 40 have  $M_{\text{vir}} > 5 \times 10^{14}h^{-1}M_{\odot}$  and 30 have  $M_{\text{vir}} > 10^{15}h^{-1}M_{\odot}$ .

For a first set of hydrodynamic simulation the mass of each DM particle in the high-resolution region is  $m_{\text{DM}} \simeq 8.47 \times 10^8 h^{-1}M_{\odot}$ , with  $m_{\text{gas}} \simeq 1.53 \times 10^8 h^{-1}M_{\odot}$  for the initial mass of gas particles. Simulations have been carried out using a Plummer-equivalent softening length for the computation of the gravitational force in the high-resolution region which is fixed to  $\epsilon = 5h^{-1}\text{kpc}$  in physical units at redshift  $z < 2$ , while being kept fixed in comoving units at higher redshift. As for the computation of hydrodynamic forces, we assume the SPH smoothing length to reach a minimum allowed value of  $0.5\epsilon$ . These simulations include radiative cooling and heating/cooling from a spatially uniform and evolving UV background. Gas particles above a given threshold density are treated as multiphase, so as to provide a sub-resolution description of the interstellar medium, according to the model described by Springel & Hernquist (2003). Within each multiphase gas particle, a cold and a hot-phase coexist in pressure equilibrium, with the cold phase providing the reservoir of star formation. Kinetic feedback is implemented by giving some type-II supernova (SN) energy to gas particles in the form of kinetic energy, thus mimicking galactic ejecta powered by SN explosions. In these runs, galactic winds have a mass upload proportional to the local star-formation rate. In addition, simulations also include a description of metal production from chemical enrichment contributed by SN-II, SN-Ia and AGB stars, as described by Tornatore *et al.* (2007). Stars of different mass, distributed according to a Salpeter IMF, release metals over the time-scale determined by the corresponding mass-dependent life-times. The metallicity dependence of radiative

cooling is included by using the cooling tables by Sutherland & Dopita (1993). In these runs, the velocity of galactic ejecta is assumed to be  $v_w = 500 \text{ km s}^{-1}$ .

For a second set of collisionless N-body simulations, we increased mass resolution by a factor of 10 and correspondingly decreased the Plummer-equivalent softening length by a factor  $10^{1/3}$ .

We show in Figure 1 some examples of temperature maps of clusters simulated with hydrodynamics. The highly complex structure of the cosmological environment surrounding the cluster region is shown by the presence of filaments and overdensities that are accreted within the main cluster halos.

## Applications

The cluster simulations described in the previous section have been used for the following analyses, which are presented in a number of papers already published or submitted for publication in refereed international journals, or in preparation.

FABJAN *et al.* (2011): analysis of the stability and robustness of different mass proxies based on observables to be measured through observations in the X-ray band from satellites.

CONTINI *et al.* (2011): analysis of the statistical properties of the substructures identified in the high-resolution DM simulations of galaxy clusters.

RASIA *et al.* (2011): comparison of masses of galaxy clusters as obtainable from X-ray and weak lensing observations.

ETTORI *et al.* (2011): definition of low-scatter mass proxies through suitable combinations of X-ray observables

KILLEDHAR *et al.* (2011): effect of baryons on the strong lensing statistical properties of the cluster population.

## References

- (1) BONAFEDE A. *et al.*, MNRAS, in press (arXiv:1107.0968), 2011
- (2) CONTINI E., DE LUCIA G. and BORGANI S., MNRAS, in press, 2011
- (3) ETTORI S., RASIA E., FABJAN D., BORGANI S. and DOLAG K., MNRAS, in press, 2011
- (4) FABJAN D., BORGANI S., RASIA E., BONAFEDE A., DOLAG K., MURANTE G. and TORNATORE L., MNRAS (in press, arXiv:1102.2903), 2011
- (5) KILLEDAR, M., BORGANI S. and MENEGHETTI M., in preparation, 2011
- (6) KOMATSU E. *et al.*, ApJS, **18**, 192, 2011
- (7) RASIA E., MENEGHETTI M., MARTINO R. and BORGANI S., *et al.*, submitted, 2011
- (8) SPRINGEL V., MNRAS, **364**, 1105, 2005
- (9) SPRINGEL V. and HERNQUIST L., MNRAS, **339**, 289, 2003
- (10) SUTHERLAND R. S. and DOPITA M. A., ApJS, **88**, 253, 1993
- (11) TORMEN G., BOUCHET F. R. and WHITE S. D. M., MNRAS, **286**, 865, 1997
- (12) TORNATORE L., BORGANI S., DOLAG K. and MATTEUCCI F., MNRAS, **382**, 1050, 2007

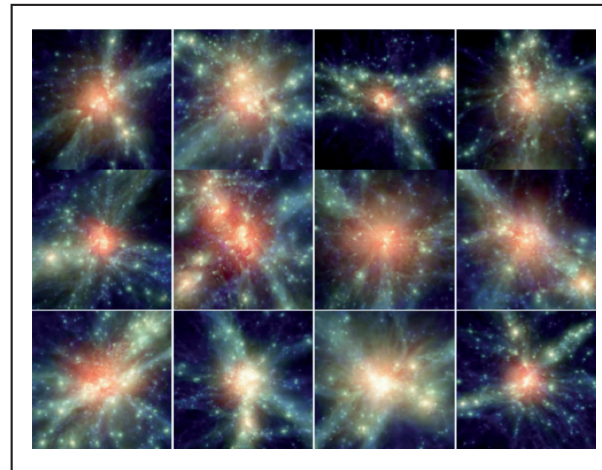


Fig. 1. – Ray-tracing images of a  $15 \text{ Mpc} \times 1$  regions around the center of the individual clusters. Color coded is the temperature of the gas, while brighter regions correspond to higher-density gas.

